



and then to convert into the B-scan sector image of the parametric map.

For the visualization and mapping we applied three signal processing algorithms: signal demodulation for echo amplitude mapping; short time Fourier transform (STFT) based algorithms for mapping of mean instantaneous frequency (MIF) and mean instantaneous bandwidth (MIB) of raw echosignal spectrum. RF signal magnitude (or instantaneous magnitude (IM)) is widely used for rendering of B type ultrasound scans. IM represents variation of RF signal envelope in time. The best way to calculate IM parameter digitally is to find the magnitude of an analytical signal:

$$x_{IM}(t) = \sqrt{x^2(t) + x_H^2(t)}. \quad (1)$$

where  $x(t)$  is the real part and  $x_H(t)$  – the imaginary part of analytical signal  $x_A = x(t) + jx_H(t)$ . Real part is the acquired signal while imaginary part is calculated using the Hilbert transform [8]:

$$x_H(t) = \frac{1}{\pi} \int_{-\infty}^{\infty} \frac{x(\tau)}{t - \tau} d\tau. \quad (2)$$

Logarithmic values of IM were used for the modulation of B-scan image color and obtaining the sector image.

The MIF parameter of ultrasound RF signal was calculated according to the equation [8]:

$$f_{MIF}(t) = \int_{-\infty}^{+\infty} f \cdot STFT(t, f) df \Big/ \int_{-\infty}^{+\infty} STFT(t, f) df, \quad (3)$$

where  $STFT(t, f)$  is a short time Fourier transform of each ultrasound RF signal (raw of the matrix of captured RF B-scan). STFT's were evaluated using these empirically optimized parameters: the shape of the window - Gaussian, the length of time window - 2,5  $\mu$ s (it is equivalent to 3,87 mm in a distance scale), overlap factor of windows – 98 %.

The MIB parameter of ultrasound RF signal was evaluated according to following equation [8]:

$$f_{MIB}(t) = \sqrt{\int_{-\infty}^{+\infty} (f - f_{MIF}(t))^2 \cdot STFT(t, f) df \Big/ \int_{-\infty}^{+\infty} STFT(t, f) df}. \quad (4)$$

RF signal parameters were used for the synthesis of the parametric map. The B-scan sector image was synthesized on the PC screen using time sequences of ultrasound signal parameters (IM, MIF and MIB) of each scan line using following scan conversion equations [9]:

$$\begin{cases} x(t) = x_0 + 0,5 \cdot c \cdot t \cdot \cos(\gamma) \\ y(t) = y_0 + 0,5 \cdot c \cdot t \cdot \sin(\gamma) \end{cases} \quad (5)$$

Here  $x(t)$  and  $y(t)$  – projections of the vector following the ultrasound beam,  $x_0$  and  $y_0$  – initial coordinates,  $c$  – mean ultrasound velocity in the eye tissues (assumed 1550 m/s),  $t$  – time,  $\gamma$  – the instantaneous angle of the ultrasound beam (assumed range of  $\gamma = \pm 25^\circ$ ).

### Evaluation of mapping results

In this section we present results of processing and

mapping using MATLAB programs. The examples of raw ultrasonic RF signal and results of it's processing are presented on Fig.2. As an example a raw ultrasound RF signal from 82-th line in B-scan is shown in top panel of Fig. 2 (a). The demodulated signal (IM) is presented in Fig. 2, (b). The software demodulated signal can be compared with the hardware demodulated signal given in bottom of original B-scan image (see Fig. 3, (a)). Strong echo pulse from the phantom target occurring at the depth of 22 mm is shown magnified on Fig.2, (c) and its amplitude spectra on Fig. 2, (d). We see significant downshift of echo central frequency from 7,5 MHz set in ultrasound system. This could be explained by influence of strong attenuation in Zerdine, which damps more higher frequencies than lower, and therefore downshift of central frequency is observed.

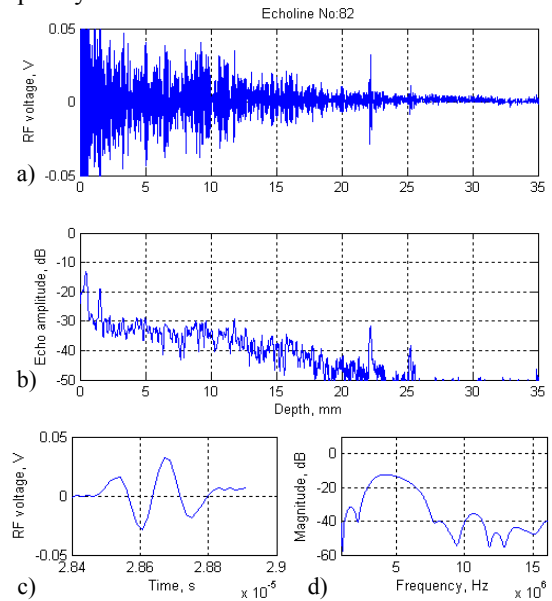


**Fig. 2.** B-scan data processing results: a – raw RF signal  $x(t)$  from line Nr.82 of B-scan; b – calculated instantaneous magnitude  $x_{IM}(t)$  of RF signal; c – pulse of echo from one-dimensional scatterer; d – amplitude spectra of echo pulse

The conventional B-scan from the screen of Mentor Advent TM A/B scanner is presented in Fig. 3 (a). The instantaneous magnitude map synthesized on the screen of PC by the developed system is presented in Fig. 4. The IM parameter based B-scan map is presented using 0,08 normalized cut-off frequency 2nd order low pass filtering and logarithmic scale. Comparison with the original B-scan image on Fig. 3 shows the visual similarity of both images.

The parametric maps of frequency parameters of ultrasound RF signal were calculated according to (3, 4) equations and are presented in Figs. 5, 6. Mapping result on Fig. 5 shows the better homogeneity of the image and better lateral resolution when compared with amplitude mapping in Fig. 4.

Fig. 6 shows 2D maps from the central phantom region in depth 21-26 mm. The region on the map corresponds with neighboring reflections from two targets, therefore from the map one can estimate the point spread function (PSF). The isolines on the echo amplitude map are drawn at levels from -34 dB to -46 dB in -3 dB intervals.

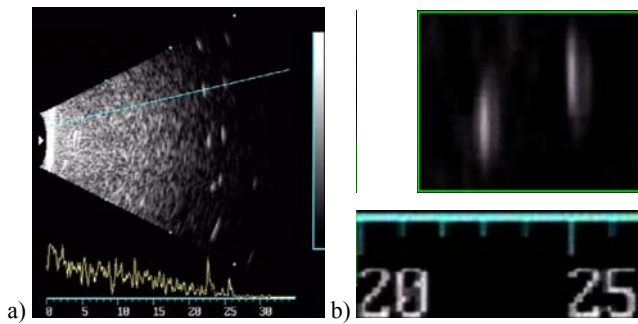


**Fig. 3.** The B scan acquired from reference points in CIRS Model 040 phantom (system acquisition parameters were: frequency 7,5 MHz, range 35 mm, gain 80 dB, velocity 1550 m/s, time gain control uniform for whole depth): a – original image; b – magnified image of points reflectors in center of B scan

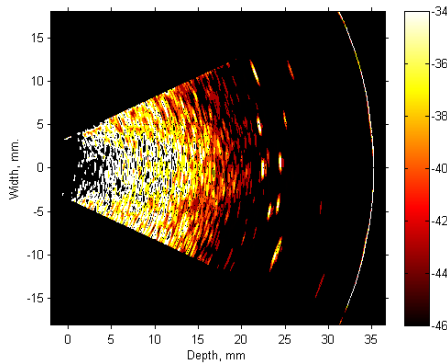


**Fig. 4.** Echo amplitude mapping result in case of phantom

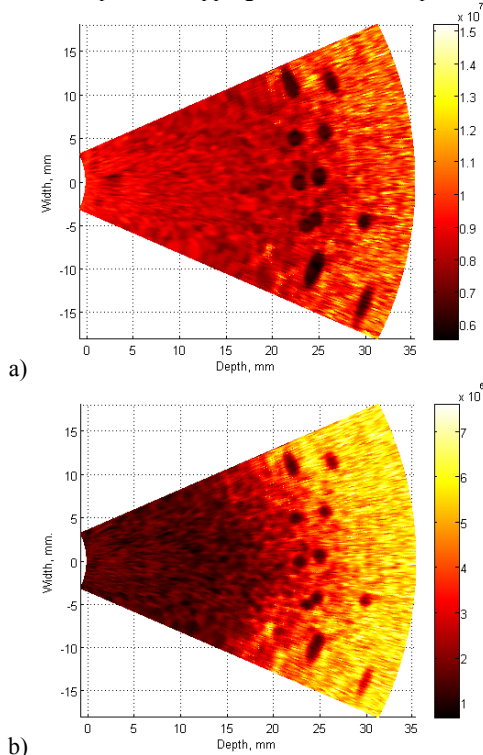


**Fig. 5.** Mapping spectral parameters of echo signal: a – mean instantaneous frequency; b – mean instantaneous bandwidth

MIB map shows isolines from 1 MHz to 3,5 MHz in intervals of 0,5 MHz. The details in amplitude and MIB maps show, that echo amplitude is the largest from start of one-dimensional target, but the MIB has minimum just after large echo amplitude. The displacement of MIB minimum from IM maximum is about 0,5 mm into the

depth. The true positions of targets are indicated with “+” signs in diagrams of Fig.6. The other interesting feature which was observed in frequency parameters maps is the different distributions of extreme values when comparing MIB and MIF maps. In the MIB map small values dominate in the area of the map where strong backscattering from Zerdine microstructure takes place and also from point reflectors. From this point of view MIB map looks similar to IM map. The MIF map shows extreme values (minimums) only from point reflectors, eliminating backscattering from Zerdine microstructure. This differentiation could be used to facilitate differentiation of point reflectors in the strong background of backscattering.

The estimated dimensions of PSF are: axial - 0,2 mm and lateral - 1,9 mm in amplitude map at -6 dB level (peak amplitude was -30 dB). In case of MIB map we see that at the level of 1 MHz dimensions of PSF are: axial - 0,9 mm, lateral - 0,8 mm. (Amplitude spectra of echo pulse from plexiglass at 20 mm depth in water helped to estimate the bandwidth of ultrasonic transducer. The measured spectrum width is 8 MHz at the level of -30 dB.) It can be observed that mapping of frequency based parameter is able to improve lateral resolution up to two times at the price of decreasing the axial resolution which becomes worse up to four times. But here should be noted that frequency based mapping gives an image containing a new information potentially valuable for tissue characterization and differentiation.

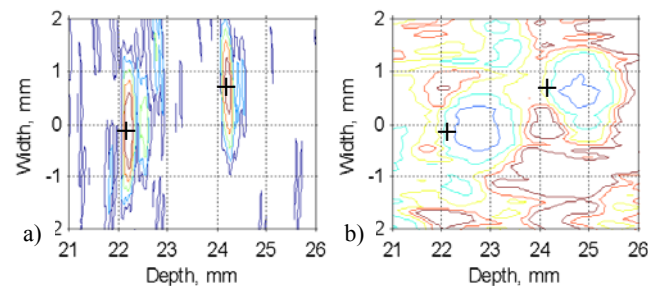


**Fig. 6.** Echo spread from one-dimensional targets in axial and lateral directions: a – mapping using IM; b – mapping using MIB

## Conclusions

Ultrasonic B-scan radiofrequency signal acquisition and processing methodology was developed and a map of frequency-related parameters was synthesized. Evaluation of map resolution and comparison with conventional B-scan images obtained from reference targets in standard phantom have shown that parametric mapping gives a qualitatively new information about frequency dependent characteristics of the tissue and at the same time the resolution of the image remains comparable with conventional amplitude based mapping. The maps obtained using mean instantaneous frequency and bandwidth of radiofrequency echoscopy signal show different resolution features. We found that lateral resolution in B-scan image could be improved twice if mapping instantaneous bandwidth instead of instantaneous amplitude. The presented mapping technology could be easily modified for the development of new parametric maps by varying the parameter calculation algorithms. Parametric maps could be used for the differential diagnostics of the tissue.

## Acknowledgment

This research was supported from Agency for International Science and Technology Development Programmes in Lithuania, EUROSTARS project E!4297 – NICDIT “A Non-Invasive Expert System for Diagnosis of Intraocular Tumours”.

## References

1. **Žakauskas M., Mačiulis A., Kopustinskas A., Paunksnis A., Kurapkienė S., Jegelevičius D.** Echospectral Methods of Tissue Evaluation // *Electronics and Electrical Engineering*. – Kaunas: Technologija, 2004. – Nr. 7(56). – P. 70–73.
2. **Paunksnis A., Kurapkienė S., Mačiulis A., Lukoševičius A., Špečkauskas M.** The use of echospectral methods of tissue evaluation for follow-up of brachytherapy treatment // *Ultrasound*. – Kaunas: Technologija, 2007. – Nr. 4(62). – P. 45–48.
3. **Coleman D. J., Silverman R. H., Rondeau M. J., Boldt H. C., Lloyd H. O., Lizzi F. L., Weingeist T. A., Chen X., Vangveeravong S., Folberg R.** Noninvasive in vivo detection of prognostic indicators for high-risk uveal melanoma: Ultrasound parameter imaging // *Ophthalmology*, 2004 March. – Vol. 111(3). – P. 558–564.
4. **Torres V.L., Allemann N., Erwenne C.M.**, Ultrasound biomicroscopy features of iris and ciliary body melanomas before and after brachytherapy // *Ophthalmic Surg Lasers Imaging*, 2005 Mar–Apr. – Vol. 36(2). – P. 129–138.
5. **John S., Sujana H., Suresh S., Swarnamani S., Biswas J., Gopal L.** Ultrasonic characterisation of malignant melanoma of choroid // *Indian J Ophthalmol*, 1998 Sep. – Vol. 46(3). – P. 153–157.
6. **Oelze M.L., Zachary J.F.** Examination of cancer in mouse models using high-frequency quantitative ultrasound // *Ultrasound in medicine & biology*, 2006. – Vol. 32(11). – P. 1639–1648.
7. **Paunksnis A., Barzdžiukas V., Kažys R.J., Raišutis R., Lukoševičius A., Paunksnis M., Janušauskas A., Marozas V., Jegelevičius D., Daukantas S., Kopsala S., Kurapkienė S., Kriauciūnienė L., Jurkonis R.** A non-invasive expert system for diagnosis of intraocular tumours: the system concept // *Ultrasound*. – Kaunas: Technologija, 2008. – Nr. 4(63). – P. 66–72.
8. **Auger F., Flandrin P., Lemoine O., Goncalves P.** The Time-Frequency Toolbox, <<http://tftb.nongnu.org>>. Accessed 2008 Dec 7.
9. **Домаркас В.Й., Пилецкас Э.Л.** Ультразвуковая эхоскопия // Ленинград: Машиностроение, 1988. – 276 p.
10. **General Purpose Multi-Tissue Ultrasound Phantom**, Model 040, User Guide & Technical Information, Rev.06/17/08 // CIRS, Inc., Norfolk, Virginia, USA
11. **Fujii Y., Taniguchi N., Itoh K., Shigeta K., Wang Y., Tsao J.-W., Kumasaki K., Itoh T.** A New Method for Attenuation Coefficient Measurement in the Liver: Comparison With the Spectral Shift Central Frequency Method // *J Ultrasound Med*, 2002. – No. 21. – P. 783–788.

Received 2009 02 26

## **R. Jurkonis, S. Daukantas, A. Janušauskas, A. Lukoševičius, V. Marozas, D. Jegelevičius. Synthesis of Parametric Map from Raw Ultrasound B-Scan Data // *Electronics and Electrical Engineering*. – Kaunas: Technologija, 2009. – No. 6(94). – P. 109–112.**

There are presented results of ultrasound radio-frequency signal sampling and processing to synthesize B-scan maps and evaluate two-dimensional visualization of ultrasound signal parameters. Our source of signal was ultrasound echoscope Mentor Advent™ A/B with mechanical scanning transducer of 11 MHz. Radio-frequency signal was digitized with digitizer Picoscope 5203. Amplitude and frequency based parameters were used for mapping B-scan ultrasound images. Standard phantom with axial resolution targets was used for the evaluation of mapping performance. We conclude that the signal processing and image transformation implemented in Matlab programs provide adequate two-dimensional mapping of B-scans. The usage of mean instantaneous bandwidth of radio frequency echoscopic signals enables to improve lateral resolution. Ill. 6, bibl. 11 (in English; summaries in English, Russian and Lithuanian).

## **Р. Юрконис, С. Даукантас, А. Янушаускас, А. Лукошявичюс, В. Марозас, Д. Ягялявичюс. Синтез параметрической карты из необработанных ультразвуковых данных В-скана // *Электроника и электротехника*. – Каунас: Технология, 2009. – № 6(94). – С. 109–112.**

В статье представлены результаты дискретизации и обработки ультразвуковых радиочастотных сигналов с целью синтезировать изображения В-скана и исследовать двумерную визуализацию параметров ультразвуковых сигналов. Источником ультразвуковых сигналов был эхоскоп Mentor Advent™ A/B с преобразователем механического сканирования на 11 МГц. Сигналы оцифровывались с помощью устройства Picoscope 5203. Разрешающая способность исследовалась при помощи стандартного фантома. На изображении В-скана были представлены не только амплитудные, но и частотные параметры эхосигналов. Работа позволяет сделать вывод, что программы обработки сигналов и трансформация изображения, реализованные в среде MATLAB, позволяют получить хорошие двухмерные карты В-сканов. Применение параметров моментной частотной полосы спектра эхоскопических сигналов позволило улучшить поперечное разрешение. Ил. 6, библи. 11 (на английском языке; рефераты на английском, русском и литовском яз.).

## **R. Jurkonis, S. Daukantas, A. Janušauskas, A. Lukoševičius, V. Marozas, D. Jegelevičius. Parametrinių vaizdų sintezė naudojant neapdorotus ultragarsinius B skenavimo duomenis // *Elektronika ir elektrotechnika*. – Kaunas: Technologija, 2009. – Nr. 6(94). – P. 109–112.**

Pateikiami ultragarsinių radijo dažnių signalų skaitmeninimo ir apdorojimo rezultatai siekiant sintezuoti B skenavimo vaizdus ir įvertinti dvimatį ultragarsinių signalų parametrų vaizdavimą. Signalo šaltinis buvo ultragarsinė echoskopinė sistema Mentor Advent™ A/B su 11 MHz mechaninio skenavimo keitikliu. Radijo dažninis signalas buvo skaitmenintas skaitmenikliu Picoscope 5203. Įvertintos dvimačio vaizdavimo galimybės tiriant išilginio skiriamumo taikinius standartiniame fantome. B skenavimo vaizduose parodytos ne tik amplitudinės, bet ir dažninės echosignalo savybės. Šis tyrimas parodė, kad apdorojant signalus ir transformuojant vaizdus Matlab terpėje galima gauti adekvačius dvimačius B skenavimo vaizdus. Naudojant radijo dažninio echoskopinio signalo vidutinį momentinį juostos plotį, galima pagerinti skersinį skiriamumą. Il. 6, bibl. 11 (anglų kalba; santraukos anglų, rusų ir lietuvių k.).

DOI: 10.5755/j02.eie.10118